Published in final edited form as:
J Magn Reson Imaging. 2012 March ; 35(3): 737–744. doi:10.1002/jmri.22848.

Polydisulfide Manganese(II) Complexes as Non-Gadolinium Biodegradable Macromolecular MRI Contrast Agents

Zhen Ye[1,2], **Eun-Kee Jeong**[3], **Xueming Wu**[1], **Mingqian Tan**[1], **Shouyu Yin**[1], and **Zheng-Rong Lu**[1,*]

[1]Department of Biomedical Engineering, Case Western Reserve University, Cleveland, OH 44106

[2]Department of Pharmaceutics and Pharmaceutical Chemistry, University of Utah, Salt Lake City, UT 84108

[3]Department of Radiology, University of Utah, Salt Lake City, UT 84108

Abstract

Purpose—To develop safe and effective manganese(II) based biodegradable macromolecular MRI contrast agents.

Materials and Methods—In this study, we synthesized and characterized two polydisulfide manganese(II) complexes, Mn-DTPA cystamine copolymers and Mn-EDTA cystamine copolymers, as new biodegradable macromolecular MRI contrast agents. The contrast enhancement of the two manganese based contrast agents were evaluated in mice bearing MDA-MB-231 human breast carcinoma xenografts, in comparison with $MnCl_2$.

Results—The T_1 and T_2 relaxivities were 4.74 and 10.38 $mM^{-1}s^{-1}$ per manganese at 3T for Mn-DTPA cystamine copolymers (M_n=30.50 kDa) and 6.41 and 9.72 $mM^{-1}s^{-1}$ for Mn-EDTA cystamine copolymers (M_n= 61.80 kDa). Both polydisulfide Mn(II) complexes showed significant liver, myocardium and tumor enhancement.

Conclusion—The manganese based polydisulfide contrast agents have a potential to be developed as alternative non-gadolinium contrast agents for MR cancer and myocardium imaging.

Keywords

Manganese(II); MRI contrast agent; biodegradable macromolecular contrast agent; cancer

INTRODUCTION

MRI is a clinical diagnostic imaging modality advantageous in providing images of soft tissues in high resolution with no ionizing radiation. Paramagnetic chelates and ferromagnetic nanoparticles are developed as MRI contrast agents to effectively improve tissue contrast by altering the relaxation rates of water protons in the tissue of interest. Currently, the most commonly used clinical contrast agents are stable Gd(III) chelates, including Gd-DTPA (Magnevist®), Gd-DOTA (Dotaram®), Gd(DTPA-BMA) (Omniscan®), Gd(DO3A-HP) (ProHance®) and Gd(BOPTA) (MultiHance®) (1,2). Recently, the Gd(III) based contrast agents have been found in association with nephrogenic systemic fibrosis (NSF), a severe disease affecting a small percentage of the patients with kidney deficiency who had a history of the exposure to Gd(III) based contrast agents (2-4).

*Correspondence to: Dr. Zheng-Rong Lu Department of Biomedical Engineering Wickenden Building, Room 427 Case Western Reserve University 10900 Euclid Avenue Cleveland, OH 44106-7207 Phone: 216-368-0187 Fax: 216-368-4969 zxl125@case.edu.

Although the cause for NSF is still unclear, the design and development of effective non-gadolinium contrast agents with lower toxicity may alleviate the safety concerns over MRI contrast agents.

Paramagnetic manganese(II) chelates or compounds are an alternative class of MRI contrast agents. As an endogenous metal, the manganese based contrast agents exhibit unique biodistribution pattern and effective contrast enhancement in the myocardium, liver and brain (5,6). Currently, two manganese based contrast agents, an oral formulation of $MnCl_2$ (Lumanhance) and an intravenous formulation of MnDPDP (Mangafordipir triosodium), are available for clinical application (5). The main limitation of the manganese based contrast agents is their relatively low relaxivities. Because of this, an increased dose is often needed to generate sufficient contrast enhancement. However, a high dose of contrast agents may lead to unexpected toxic side effects. Chemical modifications of manganese based contrast agents may result in more effective non-gadolinium contrast agents by improving their relaxivities and optimizing their pharmacokinetics and biodistribution (7-11).

Recently, we have designed and developed polydisulfide Gd(III) chelates as biodegradable macromolecular MRI contrast agents (12,13,14) to address the safety issue associated with long accumulation of macromolecular contrast agents. The polydisulfide Gd(III) chelates have shown increased relaxivity, prolonged circulation and preferential tumor accumulation as compared to small molecular Gd(III) chelates (15). These biodegradable macromolecular contrast agents were degraded into oligomeric Gd(III) chelates, which can be rapidly excreted via renal filtration after imaging (16). Incorporation of manganese(II) into polydisulfides may result in effective manganese-based MRI contrast agents with improved contrast enhancement at a relatively low dose. In this study, two polydisulfide Mn(II) complexes were synthesized and evaluated as nongadolinium biodegradable macromolecular MRI contrast agents. In vivo contrast enhancement of the agents were evaluated in female nu/nu athymic mice bearing MDA-MB-231 breast cancer xenografts.

MATERIALS AND METHODS

Synthesis of contrast agents

The biodegradable macromolecular contrast agents, Mn-DTPA cystamine copolymers (MDCC) and Mn-EDTA cystamine copolymers (MECC), were synthesized by complexing Mn(II) with its polymeric ligand DTPA cystamine copolymers (DCC) and EDTA cystamine copolymers (ECC), respectively. The polymeric ligand DTPA cystamine copolymers were prepared by copolymerizing DTPA dianhydride (5.0 mmol, 1.79 g) and cystamine (5.0 mmol, 1.13 g) as previously reported (12,13). The ligand EDTA cystamine copolymers (ECC) were obtained similarly by copolymerizing EDTA dianhydride (5.0 mmol, 1.12g) and cystamine (5.0 mmol, 1.13g). $Mn(OAc)_2$ (1.5 mmol, 0.26 g) was then complexed with DTPA cystamine copolymers (1.0 mmol, 0.51 g) or EDTA cystamine copolymers (1.0 mmol, 0.41 g) in deionized water at room temperature for 2.5 hours. The final product, Mn-DTPA cystamine copolymers and Mn-EDTA cystamine copolymers, were purified by dialysis against de-ionized water using a 10 kDa molecular-weight-cut-off membrane, and then lyophilized. The molecular weight of Mn-DTPA cystamine copolymers was determined by size exclusion chromatography (SEC) on an AKTA FPLC system with a Superose™ 6 column (GE Healthcare Life Sciences). The manganese content in the copolymers was measured by inductively coupled plasma atomic emission spectroscopy (ICP-OES). The yield is approximately 45% for both Mn-DTPA cystamine copolymers and Mn-EDTA cystamine copolymers after purification. The structures of the polymeric ligands, DTPA cystamine copolymers and EDTA cystamine copolymers, were characterized using ^{1}H-NMR and FT-IR. DTPA cystamine copolymers: ^{1}H-NMR (300 MHz, D_2O, 25°C): 2.60-2.8 (t, 4H), 2.75-3.0 (s, 4H), 3.05-3.10 (t, 4H), 3.10-3.18 (s, 4H), 3.18-3.30 (s, 4H), 3.35-3.45 (t,

4H), 3.55-3.66 (s, 2H); FR-IR: 2720-3800 cm^{-1} (ν_{O-H}), 1480-2000 cm^{-1} ($\nu_{C=O}$), 1200-1480 cm^{-1} (δ_{O-H}, ν_{C-O} and ν_{C-N}). EDTA cystamine copolymers: ^{1}H-NMR (300 MHz, D_2O, 25°C): 2.65-2.8 (t, 4H), 3.0-3.2 (s, 4H), 3.35-3.50 (s, 8H), 3.55-3.70 (s, 4H); FT-IR: 2800-3680 cm^{-1} (ν_{O-H}), 1440-1880 cm^{-1} ($\nu_{C=O}$), 1200-1480 cm^{-1} (δ_{O-H}, ν_{C-O} and ν_{C-N}). Both Mn-DTPA cystamine copolymers and Mn-EDTA cystamine copolymers were further characterized by FT-IR. Mn-DTPA cystamine copolymers FR-IR: 2640-3600 cm^{-1} (ν_{O-H}), 1480-1760 cm^{-1} ($\nu_{C=O}$), 1200-1480 cm^{-1} (δ_{O-H}, ν_{C-O} and ν_{C-N}). Mn-EDTA cystamine copolymers FT-IR: 2640-3600 cm^{-1} (ν_{O-H}), 1440-1720 cm^{-1} ($\nu_{C=O}$), 1200-1480 cm^{-1} (δ_{O-H}, ν_{C-O} and ν_{C-N}).

Kinetic stability

Calcium can replace Mn(II) from manganese complexes *in vivo* due to their structure similarity, causing the release of Mn^{2+}. The kinetic stability of Mn-DTPA cystamine copolymers and Mn-EDTA cystamine copolymers in the presence of Ca^{2+} was investigated *in vitro* by ultrafiltration as recently reported (17). Briefly, Mn-DTPA cystamine copolymers (0.71 mM-Mn) or Mn-EDTA cystamine copolymers (0.71 mM-Mn) was incubated with $CaCl_2$ (2 mM) in aqueous solution at physiological pH under room temperature for 1 hr. The solution was then transferred to the sample reservoir of a centrifugal filter (Amicon Ultra®, 3000 Da molecular weight cut-off), and centrifuged at 4000 rpm and 25 °C for 20 min. The released Mn^{2+} could be filtered through the membrane, and thus separated from the polymer bound Mn(II). The concentration of Mn(II) and Ca(II) in the pre-filtered solutions and the filtrates were determined by ICP-OES. Aqueous solutions of the polymers (0.71 mM-Mn) or $CaCl_2$ (2 mM) were used as controls. The experiments were repeated in triplicate. The degree of transmetallation was calculated as the ratio percentage of the concentration of the released Mn^{2+} in filtrate over the Mn(II) concentration before ultrafiltration.

In vitro degradation

The degradation of Mn-DTPA cystamine copolymers and Mn-EDTA cystamine copolymers was evaluated by *in vitro* incubation with cysteine. The polydisulfide Mn(II) complexes (0.71 mM-Mn) were incubated with cysteine (15 μM) in PBS buffer at physiological pH. Samples were collected before and at 15, 30, 60, 120, 360 min and 24 hr during incubation. The molecular weight of the samples were determined using SEC (AKTA FPLC system with a Superose™ 6 column, GE Healthcare Life Sciences).

Relaxivity measurement

The T_1 relaxivity of the contrast agents was determined on a Siemens Trio 3T MRI scanner. T_1 relaxation time of the aqueous solution of each contrast agent at different concentrations (0.2, 0.4, 0.6 and 0.8 mM) was measured using a saturation-recovery pulse sequence at room temperature. Data acquisition was completed at a fixed echo time (TE=11 ms) and different repetition times (TR=100, 200, 400, 800, 1600 and 3200 ms). The net magnetization (M) of each sample was measured using the software Osirix (http://www.osirix-viewer.com). T_1 was derived from the nonlinear regression equation $M = M_0(1'' e^{''TR/T_1})$ by fitting with a MATLAB software. Relaxivity was calculated as the slope of the plot of $1/T_1$ versus the concentration of Mn(II). Similarly, the T_2 relaxivity was determined using the Bruker minispec relaxometer (1.5T, 60Hz). The Mn(II) content of each sample was confirmed by ICP-OES after the MR scanning.

Animal Tumor Model

Female athymic nu/nu mice (4-6 weeks old) weighted 18-22 g were purchased from the National Cancer Institute (Frederick, MD). The animals were cared following an approved protocol and the guidelines of the local Institutional Animal Care and Use Committee. The

mice were subcutaneously implanted in both flanks with 2×10^6 MDA-MB-231 cells in a mixture of 50 μL culture medium and 50 μL Matrigel. The MRI study was performed when the tumor size reached 0.5-1.0 cm in diameter in 3~4 weeks.

Contrast Enhanced MR imaging

The contrast enhancement of polydisulfide Mn(II) complexes was investigated in female nu/nu athymic mice with MDA-MB-231 breast cancer xenografts. The mice were anaesthetized by i.p. injection of a mixture of ketamine (80 mg/kg) and xylazine (12 mg/kg). A wrist coil was used for image acquisition. The MR images were acquired on a Siemens Trio 3T MR scanner with a 3D FLASH pulse sequence (TE = 2.74 ms, TR = 7.73 ms, flip angle = 25°, slice thickness = 0.5 mm, 128×256×48 matrix size, 120 mm field of view, 0.39×0.39×0.5 mm^3 spatial resolution, 3 averages) and a 2D spin-echo sequence (TE=8.9 ms, TR=400 ms, flip angle=90°, slice thickness = 2.00 mm, 128×256 matrix size, 120 mm field of view, 0.25×0.25×2 mm^3 spatial resolution, 3 averages). Three tumor bearing mice were used for each contrast agent. The contrast agents were administered to the anesthetized mice at a dose of 0.05 mmol-Mn/kg via tail vein injection. Images were acquired before administration and at 2, 5, 10, 15, 30, 60 minutes post injection. The anesthetized mice were kept warm using a warming pad during and between image acquisitions. Signal intensity of the regions of interest (ROIs) was obtained using the Osirix software. Contrast to noise ratio (CNR) in the tumor was calculated using the equation $CNR=(S-S_0)/\sigma_n$, where S (post injection) and S_0 (thigh muscle) denote the signal within the ROIs, and σ_n are the standard deviation of random background noise. Statistical analysis was performed using a two-way ANOVA with Bonferroni's, assuming statistical significance at $p < 0.05$.

RESULTS

Synthesis of Polydisulfide Manganese(II) Complexes

The synthesis of Mn-DTPA cystamine copolymers and Mn-EDTA cystamine copolymers is described in Figure 1. The number average molecular weight (M_n) and weight average molecular weight (M_w) were 45.7 kD and 64.3 kD kDa for DTPA cystamine copolymers (polydispersity, PD = 1.4), and 156 and 255.3 kDa (PD = 1.6) for EDTA cystamine copolymers, as determined by SEC. The number average and weight average molecular weights were 30.50 and 37.35 kDa for Mn-DTPA cystamine copolymers (PD=1.2), and 61.80 and 126.37 kDa (PD = 2.0) for Mn-EDTA cystamine copolymers. The reduction of the apparent molecular weights of Mn(II) complexes was due to the decrease of the charges of the polymers after complexation and, consequently, decrease of hydrodynamic volume of the polymer complexes. The Mn(II) content in Mn-DTPA cystamine copolymers was 9.84% (w/w). The Mn(II) content in Mn-EDTA cystamine copolymers was 10.14% (w/w).

Kinetic Stability

Transmetallation, the replacement of Mn(II) ions in the chelates by endogenous metal ions, is considered as a main cause of in vivo kinetic instability for MR contrast agents based on paramagnetic metal chelates (2,3). Ca(II) ions have the same charge and similar size as Mn(II) ions, and are abundantly present in human plasma. As a result, plasma Ca(II) ions are considered as the main cause of *in vivo* transmetallation of Mn(II) complexes. Ultrafiltration was effective to separate the released and bounded Mn(II) species. In the control studies, 88.5±4.6% free Ca^{2+} ions in $CaCl_2$ aqueous solution was filtered through via ultrafiltration, while the bounded Mn(II) ions of both polymeric chelates did not filter through the membrane. Only 0.82± 1.1% Mn(II) was measured in the filtrate for Mn-DTPA cystamine copolymers, and 1.03±0.10 % for Mn-EDTA cystamine copolymers. Figure 2 shows that in the presence of $CaCl_2$, more Mn(II) (12.2±0.02%) was released from Mn-DTPA cystamine copolymers than that from Mn-EDTA cystamine copolymers (3.36±0.08%). The result

indicated that Mn-EDTA cystamine copolymers were kinetically more stable than Mn-DTPA cystamine copolymers against transmetallation with Ca^{2+} ions.

In vitro Degradation

The degradation of polydisulfides Mn(II) chelates were verified by *in vitro* incubation studies. The Mn(II) chelates were incubated in 15 μM cysteine aqueous solution (the plasma concentration of free thiols) at physiological pH. Gradual decrease of molecular weight was observed for both Mn-DTPA cystamine copolymers and Mn-EDTA cystamine copolymers, Figure 3. It appears that Mn-EDTA cystamine copolymers degraded more rapidly than Mn-DTPA cystamine copolymers. The number average molecular weights (M_n) were 30.50, 29.34, 25.60, 23.57, 21.35, 18.64 and 13.50 kDa for Mn-DTPA cystamine copolymers, and were 61.80, 56.45, 49.75, 45.36, 38.62, 32.64 and 22.57 kDa for Mn-EDTA cystamine copolymers before and at 15, 30, 60, 120, 360 and 24 hours post incubation with cysteine. Mn-DTPA cystamine copolymers were negatively charged and charge repulsion might inhibit the attack of the negatively charged cysteine at physiological pH to the disulfide bonds. In comparison, Mn-EDTA cystamine copolymers were neutral polymers and cysteine could readily react with the disulfide binds. Consequently the neutral Mn-EDTA cystamine copolymers had a faster degradation rate than Mn-DTPA cystamine copolymers in the presence of cysteine, similar to previously reported polydisulfide Gd(III) complexes (9).

Relaxivity

Figure 4 shows the MR images of the aqueous solutions of Mn-DTPA cystamine copolymers, Mn-EDTA cystamine copolymers and $MnCl_2$ at different Mn(II) concentrations acquired using the inversion-recovery sequence at 3T and the plot of $1/T_1$ versus Mn(II) concentration. The signal brightness at the same Mn(II) concentration was in the order of Mn-EDTA cystamine copolymers > Mn-DTPA cystamine copolymers > $MnCl_2$. The longitudinal relaxivity (r_1) was 2.4, 4.74 and 6.41 $mM^{-1}s^{-1}$ per Mn(II) for $MnCl_2$, Mn-DTPA cystamine copolymers and Mn-EDTA cystamine copolymers, respectively. The r_2 relaxivity was 10.38 and 9.72 $mM^{-1}s^{-1}$ for Mn-DTPA cystamine copolymer and Mn-EDTA cystamine copolymer.

In vivo MR imaging

Figure 5 shows the T_1-weighted coronal MR images of mice bearing MDA-MB-231 human breast carcinoma xenografts before and after intravenous injection of $MnCl_2$, Mn-DTPA cystamine copolymers and Mn-EDTA cystamine copolymers. The agents resulted in similar *in vivo* enhancement pattern, where significant enhancement was observed in the liver, blood pool, myocardium and bladder. The strong and prolonged liver enhancement was observed for all three agents. The polydisulfide Mn(II) complexes resulted in significant blood pool enhancement at 2 minutes post injection and the blood signal decreased afterwards. The $MnCl_2$ control resulted in little blood pool enhancement, but significant enhancement in the myocardium during the period of experiment. Substantial myocardium enhancement was also observed for the polymeric agents at 10 minutes post injection and lasted throughout the period of the experiment. Contrast enhancement in the urinary bladder increased for Mn-DTPA cystamine copolymers at 20 minutes postinjection and for Mn-EDTA cystamine copolymers at 5 minutes post-injection. No signal enhancement was observed in the bladder for $MnCl_2$ during the period of experiment. The results indicates that the polydisulfide Mn(II) complexes could be degraded and excreted via renal filtration. EDTA cystamine copolymers excreted more rapidly due to its rapid in vivo degradation even though the agent had a high molecular weight.

Figure 6 shows the axial T_1-weighted 2D spin-echo MR images of the tumor before and at different time points after injection of the agents. Slight enhancement was observed in the

tumor with $MnCl_2$ and Mn-DTPA cystamine copolymers. Mn-EDTA cystamine copolymers resulted in more significant tumor enhancement than Mn-DTPA cystamine copolymers. Quantitative analysis of the contrast-to-noise ratio in the tumor periphery showed that Mn-EDTA cystamine copolymers resulted in more significant tumor enhancement than Mn-DTPA cystamine copolymers and $MnCl_2$ for at least 1 hour, Figure 7.

DISCUSSION

In this study, we aim to develop Mn(II) based biodegradable macromolecular contrast agent as an alternative for Gd(III) based contrast agents. Two types of polydisulfide Mn(II) complexes, Mn-DTPA cystamine copolymer and Mn-EDTA cystamine copolymer, were synthesized and evaluated. The polymeric ligands were synthesized based on reported protocol, followed by Mn(II) complexation. After chelation, both polydisulfide Mn(II)-DTPA and Mn(II)-EDTA chelates showed decreased molecular weight and change in IR spectrum. The hydrodynamic volume of Mn(II) complexes appeared smaller because the polymer become nonionic after chelation. From the IR spectrum, red shift of was observed with vibration peak of C=O (from 1480-2000 to 1480-1760 for DTPA based Mn(II) chelates, and 1440-1880 to 1440-1720 for EDTA based Mn(II) chelates). In addition, significant bond weakening of the vibration of C-O and C-N (1200-1480) were observed for both Mn(II)-EDTA cystamine copolymer and Mn(II)-DTPA cystamine copolymer, indicating the contribution of the carbonyl oxygen, carboxylic oxygen and tertiary nitrogen for Mn(II) complexation.

The polydisulfide Mn(II) complexes, Mn-DTPA cystamine copolymers and Mn-EDTA cystamine copolymers, have shown some interesting features as compared to $MnCl_2$ as MRI contrast agents. The T_1 relaxivity of the polydisulfide Mn(II) complexes was increased as compared to that of $MnCl_2$ due to the increase of molecular size. The macromolecular agents had large size and hydrodynamic volume, which significantly prolonged their rotational tumbling time, resulting in relaxivity increase. Although free manganese(II) ions might have more water molecules in the inner coordination sphere, the results in this study implies that the structure and size of the agents had a stronger impact on the relaxivity of the contrast agents than a large number of water molecules in the inner sphere (18). Recent studies have shown that the water exchange rate of manganese complexes was significantly faster than that of the gadolinium chelates, compensating the lower intrinsic paramagnetism of manganese (19). Consequently, the r_1 relaxivity of the polydisulfide Mn(II) complexes was comparable to that of polydisulfide gadolinium(III) complexes, Gd-DTPA cystamine copolymers (GDCC), at 3T (20).

Mn-EDTA cystamine copolymers (6.41 $mM^{-1}s^{-1}$) had higher r_1 relaxivity than Mn-DTPA cystamine copolymers (4.74 $mM^{-1}s^{-1}$). Although the former had higher molecular weight, the size of polydisulfides might not be the main cause of difference in relaxivity of the agents based on our previous observation on the polydisulfide Gd(III) complexes (15,21). The high relaxivity of Mn-EDTA cystamine copolymers might be attributed to the low coordination number of EDTA bisamides in the copolymers, which might result in more rapid water exchange of the chelates. The chelating groups are 6 and 8 for the EDTA bisamide and DTPA bisamide in the polydisulfides, respectively. The coordination number of Mn(II) ions was up to 7 (22,23), larger than the number of chelating groups in EDTA bisamide. One coordination site from Mn(II) was available for water complexation in Mn-EDTA cystamine copolymers, while there was no free coordination site from the Mn(II) complex in Mn-DTPA cystamine copolymers. The availability of inner sphere water binding could be the main reason for higher relaxivity of Mn-EDTA cystamine copolymers. Similar relaxivity difference between Mn-DTPA based chelates and Mn-EDTA based chelates were also observed in other Mn(II) based contrast agents (7,24)

In comparison with Gd(III) chelates (log $K_{Gd\text{-}DTPA}$=17.35, log $K_{Gd\text{-}DOTA}$=22.46), Mn(II) chelates (log $K_{Mn\text{-}EDTA}$=13.9, log $K_{Mn\text{-}DTPA}$=15.2) are thermodynamically less stable, generating more concerns on transmetallation and *in vivo* metal release. Ca^{2+} is structurally similar to Mn^{2+}, and is viewed as the major cause of *in vivo* transmetallation for Mn(II) chelates (6). Although the thermodynamic stability of Mn-DTPA chelates are higher than the Mn-EDTA chelates, our kinetic stability study showed that Mn(II)-EDTA cystamine copolymers were more stable against Ca^{2+} transmetallation than Mn(II)-DTPA cystamine copolymers. After 1 hr incubation with Ca^{2+} under plasma concentration, less Mn^{2+} was released from Mn(II)-EDTA cystamine copolymers (3.36±0.08 %) than that from the Mn(II)-DTPA cystamine copolymers (12.2±0.02 %). The kinetic stability of metal chelates are generally affected by complicated factors. In our case, the higher kinetic stability of Mn(II)-EDTA based polymers may be attributed to a favorable stereochemistry of the EDTA based polymeric ligands.

Polydisulfide Mn(II) complexes resulted in less contrast enhancement in the blood pool as compared to polydisulfide Gd(III) complexes reported in our previous studies (9,10). Significant blood pool enhancement was observed in the first two minutes for the manganese based agents and then quickly disappeared, even for Mn-EDTA cystamine copolymers of high molecular weight. In contrast, Gd-DTPA cystamine copolymers with similar r_1 relaxivity and molecular weight resulted in more prolonged blood pool contrast enhancement (15). Polydisulfide Mn(II) complexes also resulted in strong and prolonged contrast enhancement in the liver, while Gd-DTPA cystamine copolymers had much less contrast enhancement in the liver. Strong liver enhancement of polydisulfide Mn(II) complexes indicated liver affinity and high liver accumulation of the agents. The liver accumulation of this agent may be attributed to favorable hepatic uptake of Mn(II). High and rapid liver accumulation of the agents could significantly reduce their concentration in the blood, consequently low blood pool enhancement.

Mn-EDTA cystamine copolymers resulted in more prominent tumor enhancement than $MnCl_2$ and Mn-DTPA cystamine copolymers in T_1 weighted 2D spin-echo MR images. However, the polydisulfide Mn(II) chelates generated less tumor enhancement than polydisulfide Gd(III) complexes (15,21). This could be attributed to the relatively low stability and high liver accumulation of the Mn(II) complexes. Between the tested Mn(II) based agents, Mn-EDTA cystamine copolymers had larger molecular weight, higher relaxivity and stability against transmetallation with Ca^{2+}, and resulted in more significant tumor contrast enhancement. The polydisulfide Mn(II) complexes also facilitated the excretion of the agents via renal filtration, as evidenced by strong bladder enhancement at 60 minutes after the injection, while little $MnCl_2$ was excreted via renal filtration.

The design and development of Mn(II) based MRI contrast agents have recently attracted a significant amount of attention because of the better safety profiles of residual Mn(II) ions (25,26). We have shown in this study that polydisulfide Mn(II) complexes had better relaxivity, pharmacokinetics, clearance and in vivo enhancement than $MnCl_2$. In comparison to some recently reported dendritic agents and colloidal systems (7-11, 26), our polydisulfide based Mn(II) contrast agents, designed to passively target tumor, showed relatively higher relaxivity and favorable pharmacokinetics. However, the main limitation of currently available Mn(II) complexes is their low complexation stability, including both thermodynamic and kinetic stabilities. Further studies are needed to design Mn(II) chelates with high thermodynamic and kinetic stability in order to develop novel Mn(II) based contrast agents and to expand their application in MR imaging of other tissues and organs. The magnetic property of Mn(II) based agents are also different from that of Gd(III)-based contrast agents. Mn(II) complexes often have much higher T_2 relaxivity, which can significantly reduce the signal in T_1-weighted imaging. This could be overcome by

designing better imaging sequence to reduce T_2 effect in T1-weighted MRI in the future studies.

In conclusion, two polydisulfide Mn(II) complexes were synthesized as gadolinium free biodegradable macromolecular MRI contrast agents. The macromolecular Mn(II) complexes readily degraded in the presence of endogenous free thiols. Both polydisulfide Mn(II) complexes had similar r_1 relaxivity as polydisulfide Gd(III) complexes, higher than that of $MnCl_2$. Mn-EDTA cystamine copolymers had higher stability than Mn-DTPA cystamine copolymers against transmetallation with Ca^{2+} ions. Similar to other reported Mn(II) chelates, polydisulfide Mn(II) complexes resulted in prominent contrast enhancement in the liver and myocardium. Macromolecular Mn(II) complexes have a potential to be developed as effective contrast agents for MR imaging.

Acknowledgments

The research work is supported in part by the NIH grant R01 EB00489.

Reference

1. Caravan P, Ellison JJ, McMurry TJ, Lauffer RB. Gadolinium(III) Chelates as MRI Contrast Agents: Structure, Dynamics, and Applications. Chem Rev. 1999; 99:2293–2352. [PubMed: 11749483]
2. Aime S, Caravan P. Biodistribution of gadolinium-based contrast agents, including gadolinium deposition. J Magn Reson Imaging. 2009; 30:1259–1267. [PubMed: 19938038]
3. Kribben A, Witzke O, Hillen U, Barkhausen J, Daul AE, Erbel R. Nephrogenic systemic fibrosis: pathogenesis, diagnosis, and therapy. J Am Coll Cardiol. 2009; 53:1621–1628. [PubMed: 19406336]
4. Kuo PH. Gadolinium-containing MRI contrast agents: important variations on a theme for NSF. J Am Coll Radiol. 2008; 5:29–35. [PubMed: 18180006]
5. Lee JH, Koretsky AP. Manganese enhanced magnetic resonance imaging. Curr Pharm Biotechnol. 2004; 5:529–537. [PubMed: 15579042]
6. Silva AC, Lee JH, Aoki I, Koretsky AP. Manganese-enhanced magnetic resonance imaging (MEMRI): methodological and practical considerations. NMR Biomed. 2004; 17:532–543. [PubMed: 15617052]
7. Bertin A, Steibel J, Michou-Gallani AI, Gallani JL, Felder-Flesch D. Development of a dendritic manganese-enhanced magnetic resonance imaging (MEMRI) contrast agent: synthesis, toxicity (in vitro) and relaxivity (in vitro, in vivo) studies. Bioconjug Chem. 2009; 20:760–767. [PubMed: 19368343]
8. Kobayashi H, Brechbiel MW. Dendrimer-based nanosized MRI contrast agents. Curr Pharm Biotechnol. 2004; 5:539–549. [PubMed: 15579043]
9. Pan D, Caruthers SD, Hu G, et al. Ligand-directed nanobialys as theranostic agent for drug delivery and manganese-based magnetic resonance imaging of vascular targets. J Am Chem Soc. 2008; 130:9186–9187. [PubMed: 18572935]
10. Pan D, Senpan A, Caruthers SD, et al. Sensitive and efficient detection of thrombus with fibrin-specific manganese nanocolloids. Chem Commun (Camb). 2009:3234–3236. [PubMed: 19587924]
11. Tan M, Ye Z, Jeong EK, Wu X, Parker DL, Lu ZR. Synthesis and Evaluation of Nanoglobular Macrocyclic Mn(II) Chelate Conjugates as Non-Gadolinium(III) MRI Contrast Agents. 22. Bioconjug Chem. 2011:931–937.
12. Lu ZR, Parker DL, Goodrich KC, Wang X, Dalle JG, Buswell HR. Extracellular biodegradable macromolecular gadolinium(III) complexes for MRI. Magn Reson Med. 2004; 51:27–34. [PubMed: 14705042]
13. Lu ZR, Mohs AM, Zong Y, Feng Y. Polydisulfide Gd(III) chelates as biodegradable macromolecular magnetic resonance imaging contrast agents. Int J Nanomedicine. 2006; 1:31–40. [PubMed: 17722260]

14. Lu ZR, Wu X. Polydisulfide Based Biodegradable Macromolecular Magnetic Resonance Imaging Contrast Agents. Isr J Chem. 50:220–232. [PubMed: 21331318]
15. Zong Y, Guo J, Ke T, Mohs AM, Parker DL, Lu ZR. Effect of size and charge on pharmacokinetics and in vivo MRI contrast enhancement of biodegradable polydisulfide Gd(III) complexes. J Control Release. 2006; 112:350–356. [PubMed: 16631270]
16. Feng Y, Zong Y, Ke T, Jeong EK, Parker DL, Lu ZR. Pharmacokinetics, biodistribution and contrast enhanced MR blood pool imaging of Gd-DTPA cystine copolymers and Gd- DTPA cystine diethyl ester copolymers in a rat model. Pharm Res. 2006; 23:1736–1742. [PubMed: 16850267]
17. Wu X, Jeong EK, Emerson L, Hoffman J, Parker DL, Lu ZR. Noninvasive evaluation of antiangiogenic effect in a mouse tumor model by DCE-MRI with Gd-DTPA cystamine copolymers. Mol Pharm. 2017:41–48.
18. Lauffer RB. Paramagnetic Metal Complexes as Water Proton Relaxation Agents for NMR Imaging: Theory and Design. Chem Rev. 1987; 87:901–927.
19. Zetter MS, Dodgen HW, Hunt JP. Measurement of the water exchange rate of bound water in the manganese(II)-adenosine triphosphate complex by oxygen-17 nuclear magnetic resonance. Biochemistry. 1973; 12:778–782. [PubMed: 4348018]
20. Koenig SH, Brown RD 3rd. Relaxation of solvent protons by paramagnetic ions and its dependence on magnetic field and chemical environment: implications for NMR imaging. Magn Reson Med. 1984; 1:478–495. [PubMed: 6571571]
21. Zong Y, Wang X, Jeong EK, Parker DL, Lu ZR. Structural effect on degradability and in vivo contrast enhancement of polydisulfide Gd(III) complexes as biodegradable macromolecular MRI contrast agents. Magn Reson Imaging. 2009; 27:503–511. [PubMed: 18814987]
22. Bianchi A, Calabi L, Giorgi C, et al. Thermodynamic and structural aspects of manganese(II) complexes with polyaminopolycarboxylic ligands based upon 1,4,7,10- tetraazacyclododecane (cyclen). Crystal structure of dimeric [MnL]2·2CH3OH containing the new ligand 1,4,7,10-tetraazacyclododecane-1,4-diacetate. J Chem Soc Dalton. 2001:917–922.
23. Aime S, Anelli L, Botta M, et al. Relaxometric evaluation of novel manganese(II) complexes for application as contrast agents in magnetic resonance imaging. J Biol Inorg Chem. 2002; 7:58–67. [PubMed: 11862541]
24. Troughton JS. Synthesis and Evaluation of a High Relaxivity Manganese(II)-Based MRI Contrast Agent. Inorganic Chemistry. 2009; 43:6313–6323. [PubMed: 15446878]
25. Pan D, Caruthers SD, Senpan A, Schmieder AH, Wickline SA, Lanza GM. Revisiting an old friend: manganese-based MRI contrast agents. Wiley Interdiscip Rev Nanomed Nanobiotechnol. 2010
26. Tan M, Wu X, Jeong EK, Chen Q, Parker DL, Lu ZR. An effective targeted nanoglobular manganese(II) chelate conjugate for magnetic resonance molecular imaging of tumor extracellular matrix. Mol Pharm. 2010; 7:936–943. [PubMed: 20481565]

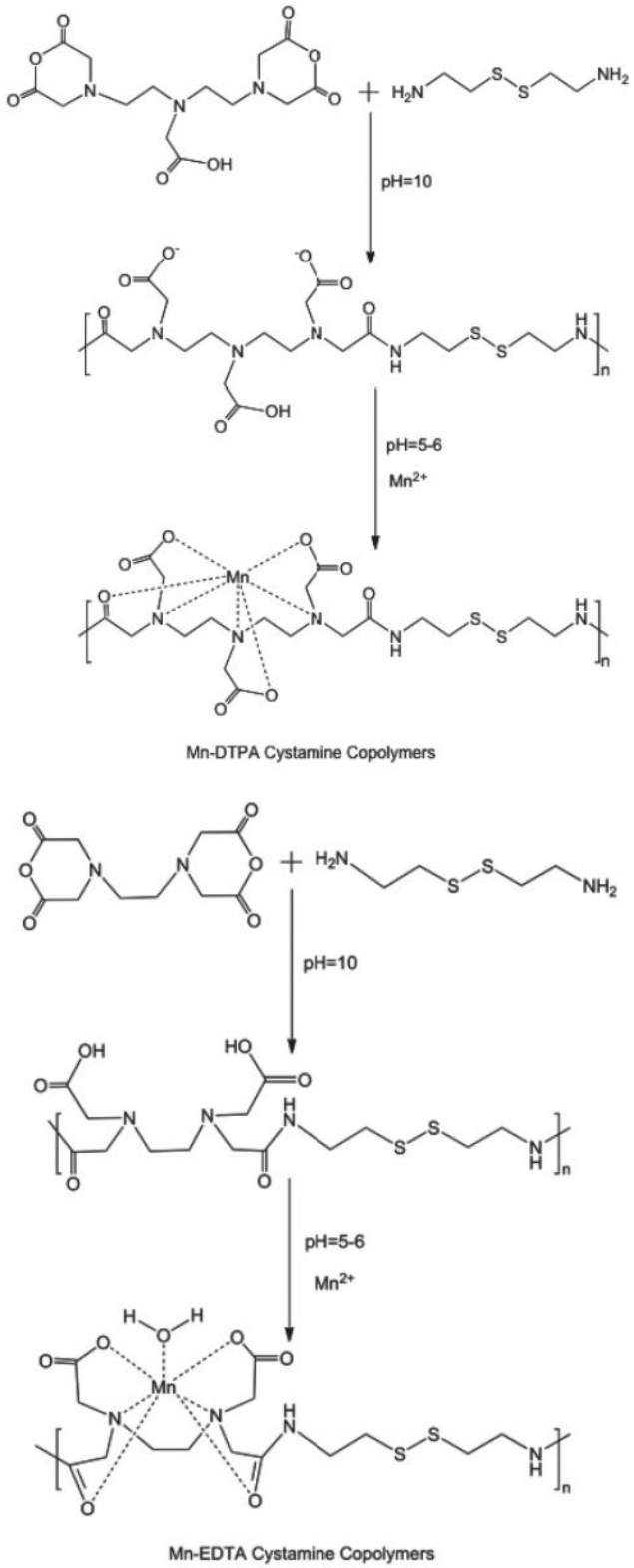

Figure 1.

Synthesis of Mn-DTPA cystamine copolymers (A) and Mn-EDTA cystamine copolymers (B).

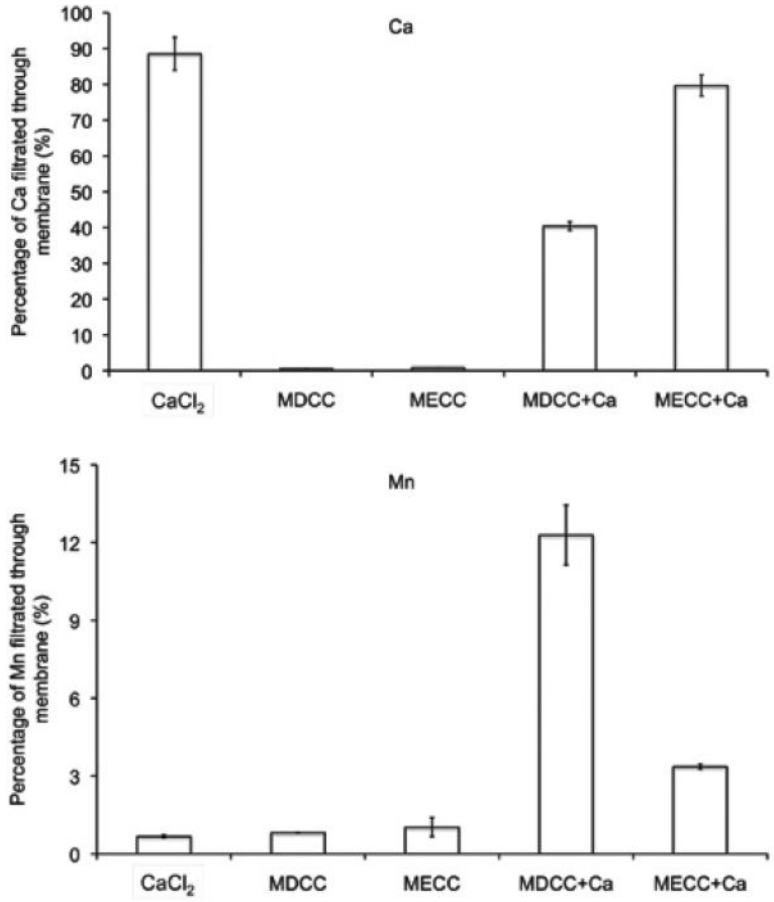

Figure 2.
Transmetallation of Mn-DTPA cystamine copolymer (MDCC), Mn-EDTA cystamine Copolymer (MECC) with Ca^{2+}.

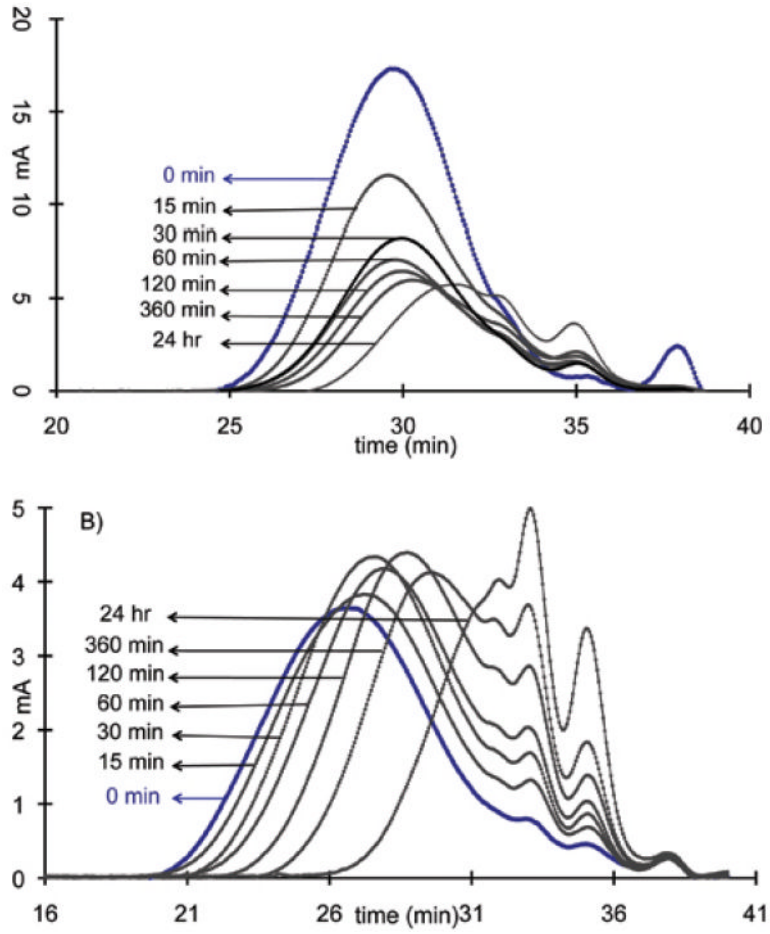

Figure 3.

The molecular weight distribution before (blue line) and at 15, 30, 60, 120, 360 and 24 hrs post incubation of the Mn-DTPA cystamine copolymer (A) and Mn-EDTA cystamine copolymer (B) against plasma concentration of cysteine (15 μM)

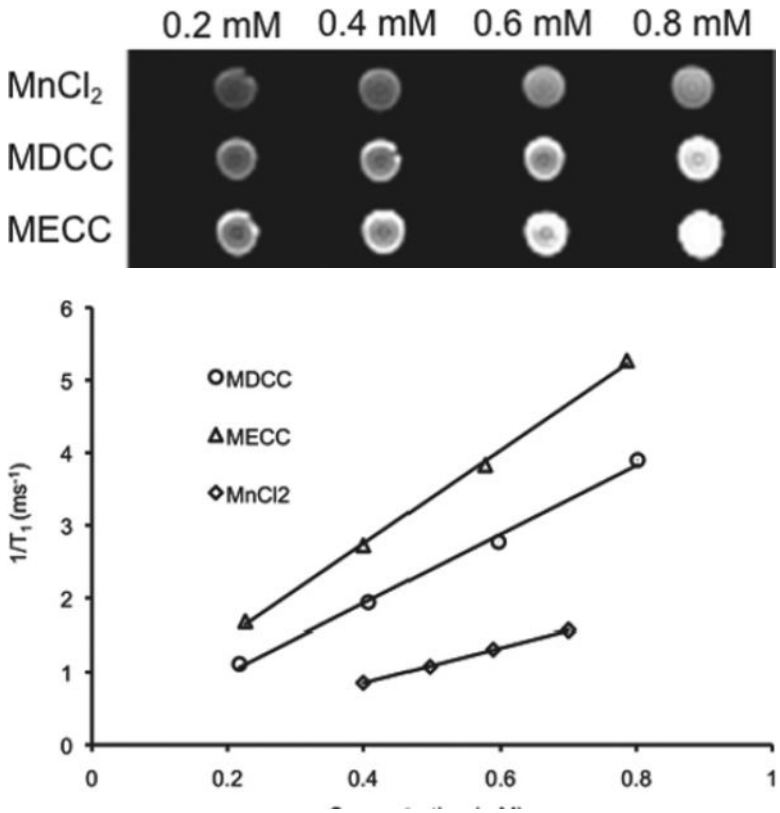

Figure 4.

(A) MR imaging of aqueous solutions of $MnCl_2$, Mn-DTPA cystamine copolymer (MDCC) and Mn-EDTA cystamine copolymer (MECC) at concentrations of 0.2, 0.4, 0.6 and 0.8 mM. (B) $1/T_1$ versus concentration plot of $MnCl_2$, MDCC and MECC for the calculation of the longiturdinal relaxation rate (R_1).

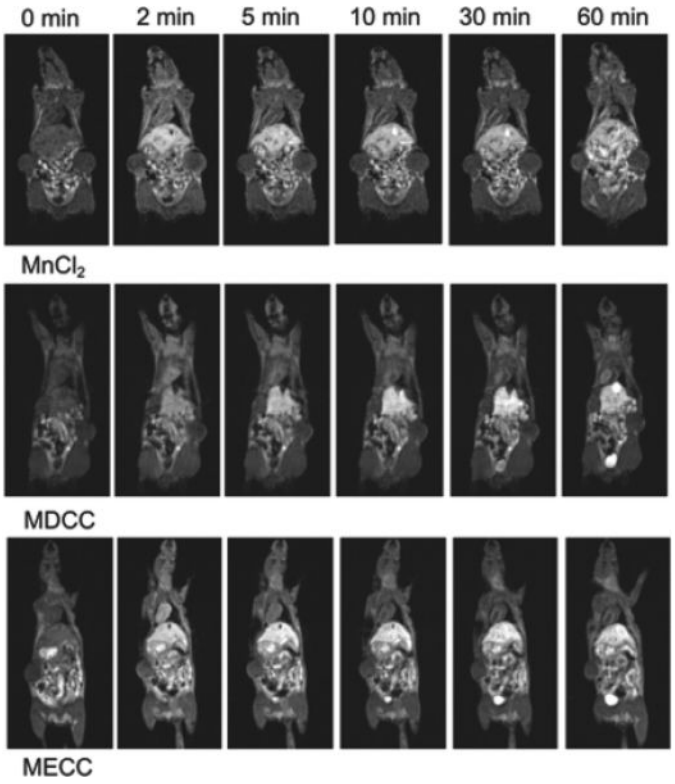

Figure 5.
3D coronal images before (0 min) and at 2, 5, 10, 30 and 60 minutes post injection of $MnCl_2$, Mn-DTPA cystamine copolymers (MDCC), and Mn-EDTA cystamine copolymers (MECC) at a dose of 0.05 mmol-Mn(II)/kg.

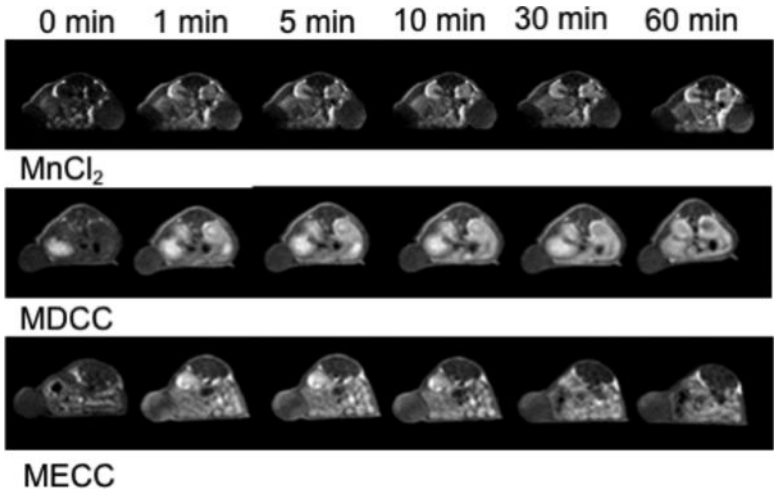

Figure 6.

2D spin echo image of the tumor before and 2, 5, 10, 30 and 60 minute after intravenous injection of $MnCl_2$, Mn-DTPA cystamine copolymers (MDCC) and Mn-EDTA cystamine copolymers (MECC) at a dose of 0.05 mmol-Mn/kg.

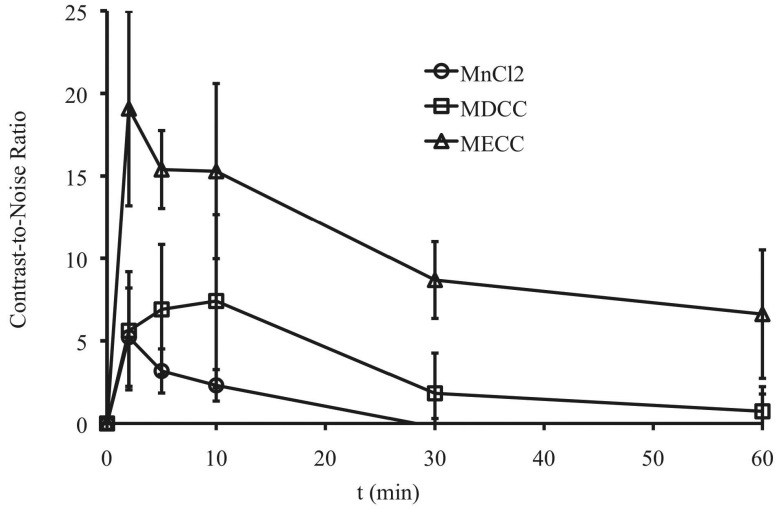

Figure 7.

Contrast-to-Noise Ratio (CNR) of tumor periphery before and at 2, 5, 10, 20, 30 and 60 minutes post tail vein injection of $MnCl_2$ (circle), Mn-DTPA cystamine copolymers (square), Mn-EDTA cystamine copolymers (triangle) at a dose of 0.05 mmol-Mn/kg.